PAPER

Ionic tagged amine supported on magnetic nanoparticles: synthesis and application for versatile catalytic Knoevenagel condensation in water

Anguo Ying,* Fangli Qiu, Chenglin Wu, Huanan Hu and Jianguo Yang*

Propylamine modified with imidazolium ionic moiety grafted onto magnetic nanoparticles (MNPs) was prepared and evaluated as a catalyst for Knoevenagel condensation in water at room temperature. The catalyst was efficient in the reaction to give the condensation products in good yields. It is worth noting that the ionic-tagged catalyst performed significantly better than its ionic tag-free counterpart. Finally, the catalyst could be reused for 8 times with a slight loss in its catalytic activity.

1. Introduction

The Knoevenagel condensation of aldehydes with acidic active methylene compounds represents one of the most fundamental carbon–carbon formation reactions in the field of organic transformations.[1–6] The corresponding condensation products are electrophilic trisubstituted alkenes, which have been widely used not only as starting materials for Michael addition[7] and domino or one-pot reactions,[8] but also as important intermediates for the preparation of functional polymers, fine chemicals and pharmaceutical drugs.[9] Traditionally, this type of condensation reactions are performed in homogeneous solution in the presence of organic bases as well as their salts as catalysts, including dimethylamino pyridine, piperidine, guanidine and ethylenediamine.[10] These methods are obviously limited by the difficulties of catalyst separation and recyclability. Therefore, several methodologies for the Knoevenagel condensation catalyzed by heterogeneous catalysts were developed, in which the catalysts are readily recoverable and are recycled. For example, MgO/ZnO,[11a] amine-functionalized polyacrylonitrile fiber,[11b,c] La$_2$O$_3$/MgO,[11d] Ni–SiO$_2$,[11e] Si-MCM-41 supported basic materials[11f] and IRMOF-3 (ref. 11g) have been tested to catalyze the condensation reactions. Each of the abovementioned methods has its own merits with at least one of the limitations of low yields, narrow substrate scope, harsh reaction conditions and the involvement of large amounts of harmful and toxic organic solvents. Hence, improved methods for the Knoevenagel condensation using inexpensive, readily available catalysts and less scavenger reagents coupled with easier work-up procedures are highly desirable.

Magnetic nanoparticles (MNPs) are extensively studied as efficient supports for immobilizing homogeneous catalysts for various organic transformations because of their interesting properties such as high surface area and paramagnetic properties, facilitating their separation from reaction media after magnetization with an external permanent magnetic field.[12] MNPs-supported guanidine was developed and used to catalyze the cyanosilylation of carbonyl compounds to achieve good to high yields of the desired products.[13] In addition, the nanocatalyst can be reused up to 20 times. Gawande and coworkers reported a sulfonic acid catalyst grafted on magnetite and subsequently served as a highly efficient magnetic catalyst for the Ritter and multicomponent reactions.[14] Meanwhile, a new concept of ion-tag strategy that can be achieved by installing an ionic substituent on the catalyst has been presented.[15] Catalysts optimized and designed according to the ion-tag strategy have three advantages, including water compatibility, readily recyclable and higher catalytic activities compared to the parent tag-free catalysts, which, to some extent, is a working hypothesis. Thus, a series of novel ionic tagged catalysts have emerged and have been exploited in versatile organic transformations such as aza-Michael addition,[16] selective hydroformylation,[17] olefin reduction,[18] Suzuki–Miyaura reaction,[19] asymmetric Henry reaction,[20] enantioselective α-aminoxylations of ketones and aldehydes,[21] asymmetric allylic etherification,[22] and asymmetric addition.[23] Based on the unique properties of magnetic nanoparticle support and ion tag of ionic liquid, a new model for the design of efficient and recoverable catalysts has been developed *via* the combination of magnetite and ionic liquid (Scheme 1). Consequently, with the principle for the construction of catalysts in hand and in continuation of our research endeavors on the development of environmentally benign and sustainable chemical processes,[24] herein, we report a novel MNPs supported amine with ionic tag and its application as a highly efficient and

School of Pharmaceutical and Chemical Engineering, Taizhou University, Taizhou 318000, China. E-mail: agying@tzc.edu.cn; yinganguo@163.com; yjg@tzc.edu.cn; Fax: +86 576 88660359; Tel: +86 576 88660359

Scheme 1 A model for the design of novel catalysts.

magnetically recoverable catalyst for the versatile Knoevenagel condensations.

2. Results and discussion

2.1 Preparation and characterization of catalysts

The magnetic nanoparticle supported catalyst **4** (MNPs-IT-PA) was prepared in multiple steps from several commercially available chemicals (Scheme 2). $SiO_2@Fe_3O_4$ **1** (MNPs) was synthesized by a chemical co-precipitating method reported in the literature,[25] followed by silica coating.[26] The outer silica shell can not only prevents the aggregation of nanoparticles but also provides suitable surface Si–OH groups for further functionalization.[27] *N*-(3-propyltriethoxysilane) imidazole **2** was prepared *via* the condensation of imidazole and 3-chloropropyltriethoxysilane, and was then grafted on the MNPs to give the supported imidazole **3**. Subsequently, **3** was refluxed with 3-bromine propylamine in dry toluene under nitrogen atmosphere to afford the final catalyst MNPs-IT-PA **4**. For comparison, ion-free counterpart **6** (MNPs-PA), in which 3-aminopropyltriethoxysilane **5** was directly immobilized onto the magnetic nanoparticles, was prepared, as outlined in Scheme 2.

The transmission electron microscopy (TEM) images in Fig. 1 show that MNPs (a), MNPs-PA (b) and MNPs-IT-PA (c) are uniformly sized magnetic nanoparticles with an almost spherical morphology. The diameter of the all the three kinds of particles is approximately 16 nm, which is significantly larger than naked Fe_3O_4 particles. The similar size and morphology of blank support (a) and amine anchored (b and c) implies that the immobilization process did change the magnetic ferrite core,
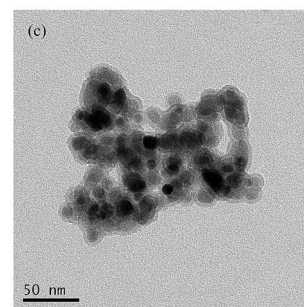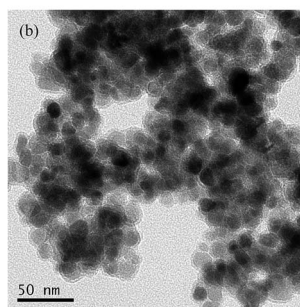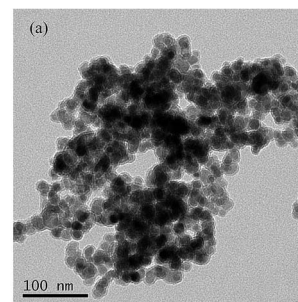
Fig. 1 TEM images of MNPs (a), MNPs–PA (b) and MNPs–IT–PA (c).

and the modification reaction for catalyst loading only occurred on the silica shell surface.

The X-ray diffraction (XRD) spectra of anchored catalysts MNPs-IT-PA, MNPs-PA and MNPs have the same typical peaks with respect to their positions and relative intensities (Fig. 2). A broad peak from $2\theta = 18°$ to $28°$ is attributed to the amorphous silica shell formed surrounding the Fe_3O_4 core.[28] The peaks at $30.07°$, $35.41°$, $43.04°$, $53.39°$, $56.91°$, and $62.49°$ correspond to the (220), (311), (400), (422), (511), and (440) reflections of the crystalline cubic spinel structure of standard naked Fe_3O_4 sample (JCPDS 19-0629), respectively. As shown in Fig. 2, the phase composition of MNPs remained intact after surface modification on nanoparticles.
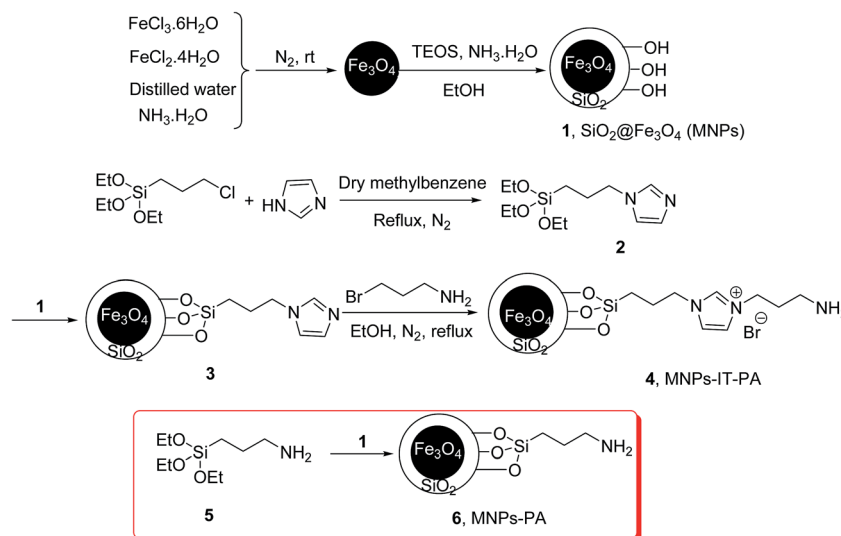
Scheme 2 Preparation of magnetic nanoparticle supported catalyst MNPs-IT-PA **4** and MNPs–PA **6**.
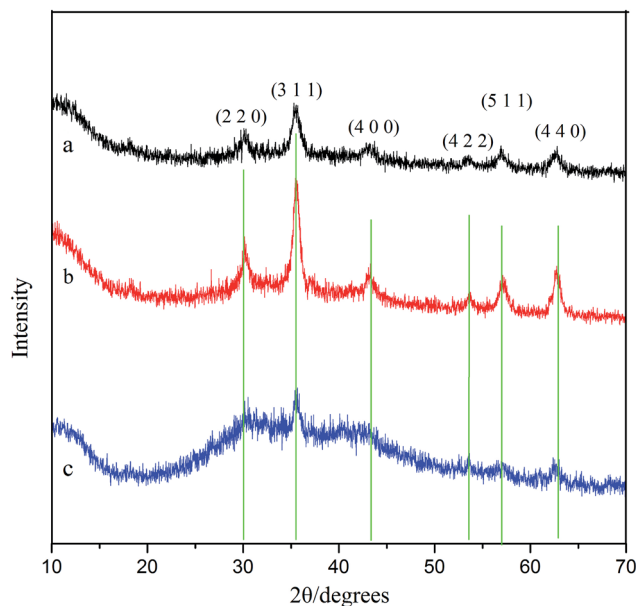
Fig. 2 XRD spectra of MNPs (a), MNPs-PA (b) and MNPs-IT-PA (c).

Successful functionalization of MNPs can be verified from the FT-IR spectra shown in Fig. 3.

In Fig. 3, the band at 579 cm^{-1} was assigned to the characteristic Fe–O vibrations and confirmed the existence of Fe_3O_4 component in all the three samples. A broad peak at around 3400 cm^{-1} is attributed to the Si–OH group. Moreover, the presence of Si–O bond in three samples is evident from two characteristic vibrations at 953 cm^{-1} and 1086 cm^{-1}. The samples b and c exhibit adsorptions at 2965 cm^{-1}, 2874 cm^{-1}, and 1465 cm^{-1}, as attributed to the C–H stretching vibration of linker 3-chloropropyltriethoxysilane anchored on the surface of $SiO_2@Fe_3O_4$.[29] The imidazole tag was responsible for the covalent anchoring of propylamine by forming an imidazolium-based ionic liquid moiety, which was evident from characteristic bands at 1507 cm^{-1} of C=N vibration and at 3143 cm^{-1} of C–H stretching on the imidazole ring,[30] as shown in Fig. 3c. Two

new bands at 1211 cm^{-1} and 1153 cm^{-1} corresponding to the N–H stretching vibration of primary amine indicate that the MNPs are functionalized with propylamine modified by imidazolium-based ionic liquid.

The magnetic properties of neat $SiO_2@Fe_3O_4$ (a), ionic-free supported amine (b) and ionic tagged amine anchored on MNPs (c) were investigated at room temperature (Fig. 4). The saturation magnetizations were 32.2, 36.4, and 56.4 emu g^{-1}, respectively. It should be noted that the high magnetization and superparamagnetism of the ionic-tagged amine loaded sample exhibits good magnetic character and re-dispersion properties, which enables the catalyst to be well-dispersed in the reaction solution and to be easily recovered by an external magnetic force (Fig. 5).

The thermal stabilities of the two immobilized catalysts were determined by thermogravimetric (TG) analysis. The results are shown in Fig. 6. The two TG curves were divided into several regions corresponding to different mass loss ranges. The first weight loss for both the samples, which occurred below 200 °C
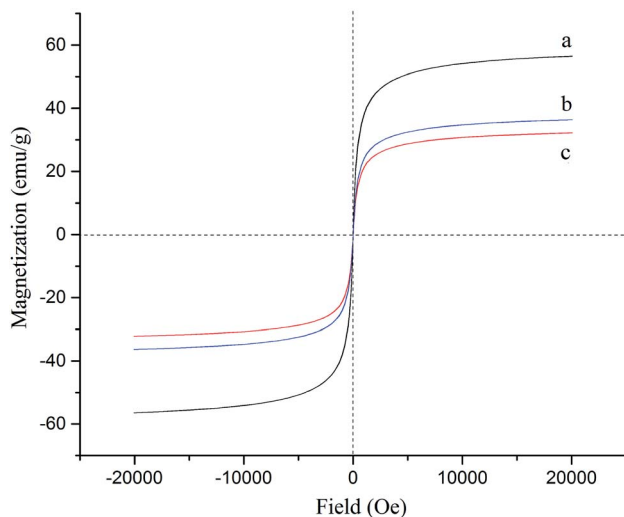
Fig. 4 Room temperature magnetization curves for MNPs (a), MNPs-PA (b) and MNPs-IT-PA (c).

Fig. 3 FT-IR spectra of MNPs (a), MNPs-PA (b) and MNPs-IT-PA (c).
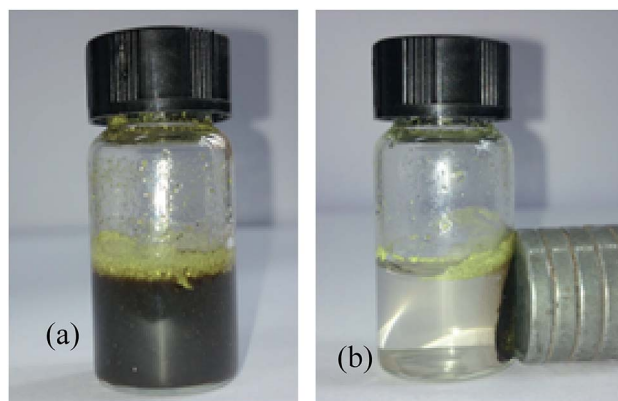
Fig. 5 Photographs of the dispersion of catalyst MNPs-IT-PA (a) and the separation of the catalyst using an external magnet.
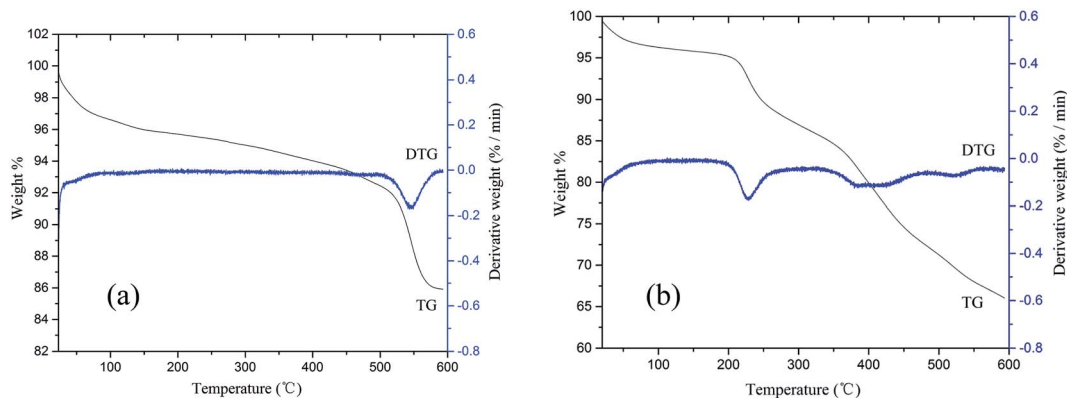
Fig. 6 TG-DTG analysis for $SiO_2@Fe_3O_4$-PA(a) and MNPs–IT–PA (b).

was probably because of the loss of adsorbed solvent or trapped water on the surface and structural water within amorphous silica outside the Fe_3O_4 core. A mass loss of approximately 4.5% of $SiO_2@Fe_3O_4$-PA occurring between 198 °C and 510 °C was attributed to the loss of propylamine. Further mass loss of the catalyst MNPs-PA at higher temperature was a result of the decomposition of silica shell (Fig. 6a).[31] For catalyst MNPs-IT-PA, the second weight loss in the range of 199 °C to 350 °C was accounted by the cleavage of imidazolium ionic liquid-modified amine, which was very obvious in the DTG curve (Fig. 6b). The occurrence of further decomposition beyond 351 °C could be designated as the complete loss of imidazolium-functionalized trialkoxysilane moiety.[32] The loading amount of propylamine and amine combined with ionic moiety were determined to be 0.21 mmol g^{-1} and 0.34 mmol g^{-1}, respectively, by elemental analysis, well in accordance with the TG analysis.

2.2 Catalytic performances in versatile Knoevenagel condensation

The catalytic activities of MNPs-PA and MNPs-IT-PA were investigated using the Knoevenagel condensation between 2-(cyanomethyl)benzimidazole (5 mmol) and 2-thenaldehyde (5 mmol). According to the results provided in Table 1, the catalyst MNPs-IT-PA performed well to give the desired product within 2 h in 79% yield, while ionic tag-free catalyst MNPs-PA gave the same desired product in 62% yield (Table 1, entries 2 and 3). The results confirmed that MNPs-IT-PA catalyzes the model reaction significantly better than its counterpart ionic tag-free MNPs-PA, which may be attributed to the improved mass transfer originating from the hydrophobic ionic moiety.[33] Only 28% yield of the product was obtained when the reaction was carried out in the presence of a blank support ($SiO_2@Fe_3O_4$) even if the reaction time was prolonged to 5 h (Table 1, entry 1).

Table 1 Evaluation of the effects of the catalyst and solvent on the Knoevenagel condensation reaction of 2-(cyanomethyl)benzimidazole and 2-thenaldehyde at room temperature
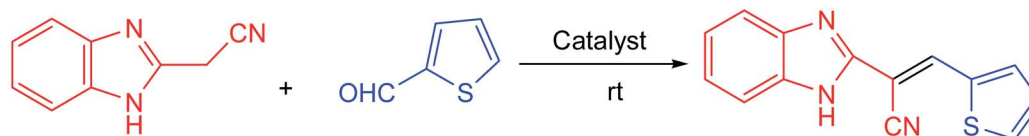
Entry	Catalyst (mol%)	Solvent (10 mL)	Time (h)	Yield (%)[a]
1	MNPs ($SiO_2@Fe_3O_4$) (73.5 mg)	H_2O	5	28
2	MNPs-PA (5.0)	H_2O	2	62
3	MNPs-IT-PA (5.0)	H_2O	2	79
4	MNPs-IT-PA (10.0)	H_2O	2	79
5	MNPs-IT-PA (20.0)	H_2O	3	80
6	MNPs-IT-PA (2.0)	H_2O	2	63
7	MNPs-IT-PA (0.5)	H_2O	3	37
8	MNPs-IT-PA (5.0)	Methanol	3	58
9	MNPs-PA (5.0)	Methanol	2	68
10	MNPs-IT-PA (5.0)	Toluene	3	52
11	MNPs-PA (5.0)	Toluene	3	65
12	MNPs-IT-PA (5.0)	CH_2Cl_2	3	57
13	MNPs-PA (5.0)	CH_2Cl_2	3	61

[a] Isolated yield.

Table 2 MNPs-IT-PA catalyzed the Knoevenagel condensation of various aromatic aldehydes with 2-(cyanomethyl)benzimidazole, 2-(cyanomethyl)benzothiazole and phenylacetonitrile and indole-2-acetonitrile[a]
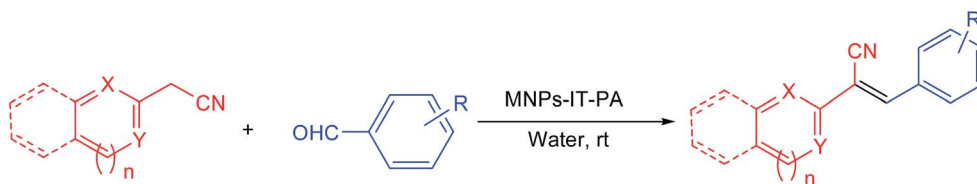
Entry	Substrate	Aldehyde	Time (h)	Yield (%)[b]
1			2	83
2			1.5	85
3			1	88
4			2	84
5			4	83
6			2	80
7			3	76
8			1.5	84
9			2	85
10			2	85
11			3	90
12			3	78

Table 2 (*Contd.*)
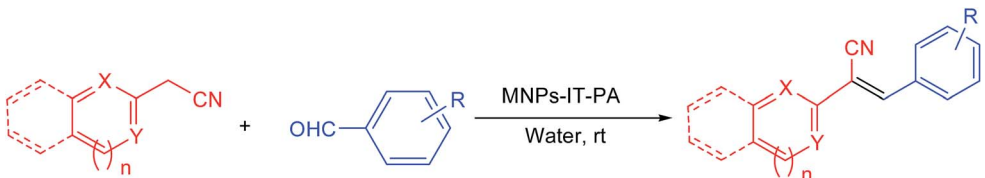
Entry	Substrate	Aldehyde	Time (h)	Yield (%)[b]
13			3	85
14			5	82
15			5	86
16			5	81
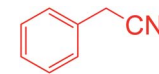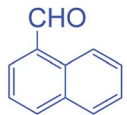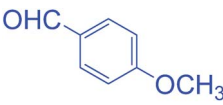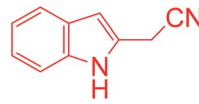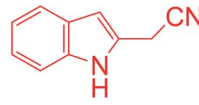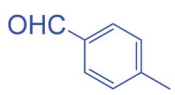
[a] Reaction conditions: methyl active compounds (5 mmol), aldehydes (5 mmol), water (10 mL), MNPs-IT-PA (5 mol%), rt. [b] Isolated yield.

The reaction conditions were further optimized at different catalyst loadings, revealing that 5 mol% of the catalyst MNPs-IT-PA afforded the best catalytic efficiency in the terms of reaction rate and yield (Table 1, entries 4–7). For comparison, several organic solvents were also exploited as media for the reaction. The reactions catalyzed by MNPs-IT-PA in methanol, toluene and dichloromethane resulted in the product with lower yields (Table 1, entries 8, 10 and 12). It is worth noting that the ionic tag-free catalyst performed better in organic solvents than the ionic-tagged catalyst MNPs-IT-PA (Table 1, entries 8–13). Considering reaction efficiency as well as the principle of green chemistry, the reaction catalyzed by MNPs-IT-PA in water at room temperature was used for further examinations.

With optimal reaction conditions in hand, we proceeded to investigate the scope of methyl active compounds and various substituted arylaldehydes, and the results are shown in Table 2. A wide range of aromatic aldehydes reacted with 2-(cyano-methyl)benzimidazole to give products in high yields (Table 2, entries 1–7). The reaction rate of aldehydes with electron-with-drawing groups at the aromatic ring is slightly faster than that with electron-donating groups (Table 2, entries 1–2 *vs.* 3–6). On the other hand, the reaction of mono-, di-, tri-substituted or 9-anthraldehyde proceeded more slowly than that of benzalde-hyde because of the steric hindrance of substitutents at the ring (Table 2, entries 1 *vs.* 3–5 and 7). Gratifyingly, 2-(cyanomethyl) benzothiazole, phenylacetonitrile and indole-2-acetonitrile were also found to be efficient methylene active ingredients to give the desired condensation products in good yields albeit

relatively longer reaction times were required for indole-2-acetonitrile (Table 2, entries 15 and 16). It is worth noting that all the obtained products were exclusively E-isomers.

Encouraged by the exciting results of cyano-substituted methylene active compounds in the present catalytic system, we also attempted to conduct the condensation of non-cyano substituted ketone (**I**) and benzaldehyde to form the product 4-methyl-3-oxo-N-phenyl-2-(phenylmethylene)pentanamide (**II**), which is a key intermediate for the preparation of Atorvastatin calcium(**III**), which can inhibit 3-hydroxy-3-methylglutaryl-coenzyme (HMG-CoA) reductase (Scheme 3).[34] To our pleasure, the reaction proceeded smoothly in the presence of catalyst MNPs-IT-PA in water, and 84% yield of the product (**II**) was achieved within 4 h (reaction condition **A** in Scheme 3). Only 59% product yield was obtained when the reaction was promoted by ionic tag-free catalyst $SiO_2@Fe_3O_4$-PA (condition **B**). The traditional method for the preparation of **III** requires a large amount of organic solvent and acid (Condition **C**). Compared with **B** and **C**, the reaction conditions **A** using ionic-tagged MNPs-IT-PA as catalyst may provide an environmentally friendly alternative route for the synthesis of Atorvastatin calcium on an industrial scale.

The obvious catalytic role of MNPs-IT-PA in Knoevenagel condensation could be attributed to two factors. As depicted in Fig. 7, nitrogen with a lone pair electron at the primary amine of MNPs-IT-PA (Function domain) could act as an acceptor to form a hydrogen bond with a methylene active ingredient. The resulting carbon anion would attack the aldehyde, followed by
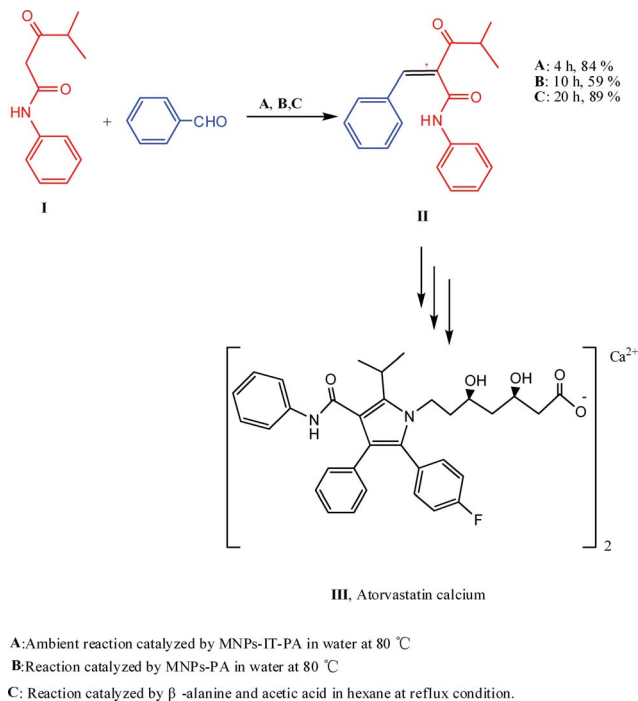
Scheme 3 Aqueous Knoevenagel condensation of non-cyano substituted ketone with benzaldehyde under various reaction conditions.

A:Ambient reaction catalyzed by MNPs-IT-PA in water at 80 ℃
B:Reaction catalyzed by MNPs-PA in water at 80 ℃
C: Reaction catalyzed by β -alanine and acetic acid in hexane at reflux condition.

A: 4 h, 84 %
B: 10 h, 59 %
C: 20 h, 89 %

III, Atorvastatin calcium
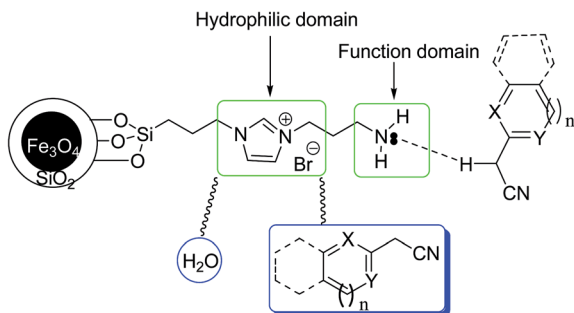
Fig. 7 Proposed explanation of MNPs-IT-PA as a catalyst for the Knoevenagel condensation.

the removal of a molecule of H_2O to provide the final condensation product. Second, the hydrophilic domain of ionic moiety in the catalyst could play the role of a phase transfer catalyst (PTC), which would increase the solubility of the reagent in water. It is clear that the poor water solubility of a methylene active compound decreases the catalytic activity of the primary amine, which was verified by ionic-free $SiO_2@Fe_3O_4$-PA promoted processes (Table 1, entry 2 *vs.* entry 3 and Scheme 3, condition A *vs.* condition B). Moreover, the "ionic environment" present electrosteric activation to stablize the transition state of the reaction.[15] Both the hydrophic property and the presence of a good acceptor on the nitrogen of MNPs-IT-PA efficiently facilitate the reaction.

One of the main advantages of the supported catalyst is its recyclability. Thus, we turned our attention to the reusability of the ionic-tagged catalyst MNPs-IT-PA. Upon the completion of
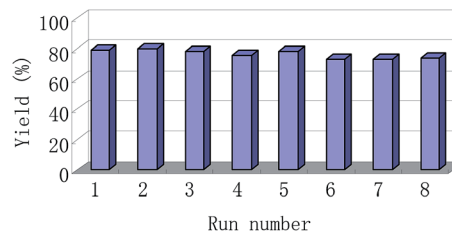
Fig. 8 Recyclability study of the catalyst MNPs-IT-PA in an aqueous reaction of 2-(cyanomethyl)benzimidazole (5 mmol) and 2-thenaldehyde (5 mmol) in water (10 mL) within 2 h.

the reaction, the magnetic catalyst was readily recovered by an external magnet (Fig. 5b), and was reused in the next run before it was successively washed with ethanol and ethyl acetate. As shown in Fig. 8, the catalyst MNPs-IT-PA could be reused for 8 times and no significant decrease in the product yield was observed. In addition, the amine loading of the catalyst subjected to 8 runs was 0.31 mmol g^{-1}, demonstrating the covalent connection between the ionic-modified amine and MNPs.

3.   Conclusions

In conclusion, the first magnetic nanoparticles supported propylamine with an ionic liquid modification was designed and prepared. The ionic-tagged supported catalyst MNPs-IT-PA was used as highly efficient promoter for the Knoevenagel condensation to afford products in good yields. Moreover, MNPs-IT-PA could also be used as a catalyst to prepare 4-methyl-3-oxo-*N*-phenyl-2-(phenylmethylene)pentanamide, which is a key intermediate for the synthesis of Atorvastatin calcium. The comparison between MNPs-IT-PA and MNPs-PA shows that the ionic moiety efficiently facilitates the reaction. The catalyst MNPs-IT-PA can be reused 8 times with a slight loss of catalytic activity.

4.   Experimental

4.1   Materials and instruments

All the chemical reagents were used without further purification. The reaction monitoring was accomplished by thin layer chromatography (TLC) on gel F254 plates. Powder X-ray diffraction data were obtained using Cu Kα radiation. Fourier transform infrared spectroscopy (FT-IR) was performed on a spectrometer using KBr pellets. Transmission electron microscopy (TEM) was performed with an instrument operating at 40–100 kV. Magnetic measurements were carried out in a vibrating sample magnetometer (VSM) at room temperature. ^1H and ^{13}C NMR were recorded on a spectrometer at 400 MHz and 100 MHz in $CDCl_3$, respectively. Chemical shifts were reported in parts per million ($δ$), relative to the internal standard of tetramethylsilane (TMS).

4.2   Preparation of silica coated magnetic nanoparticle-$SiO_2@ Fe_3O_4$ 1 (MNPs)

Magnetic (Fe_3O_4) nanoparticles were prepared by co-precipitation.[25] $FeCl_3·6H_2O$ (8.1 g, 0.03 mmol) and $FeCl_2·4H_2O$ (4.97 g,

0.025 mmol) were added to deionized water (100 mL) and sonicated until the salts dissolved completely. Then, the transparent solution was heated at 85 °C with vigorous mechanically stirring under N_2 atmosphere for 1 h. pH was then adjusted to 9 using concentrated aqueous ammonia (25 wt%). The black precipitate was washed several times with deionized water until the pH of the eluent decreased to 7. The coating of a layer of silica on the surface of the naked Fe_3O_4 was achieved by the sol–gel method.[26] The naked Fe_3O_4 (1.0 g) was diluted with ethanol (200 mL) by ultrasonic irradiation. 6 mL concentrated $NH_3 \cdot H_2O$ and 2 mL of tetraethoxysilane (TEOS) were added to the well-dispersed magnetic nanoparticles solution and stirred for 24 h at room temperature. The resulting MNPs **1** was collected by an external magnet and washed with water until the solution was neutral. Then, it was washed with ethanol and diethyl ether successively and dried under vacuum.

4.3 Synthesis of the catalysts MNPs-IT-PA and MNPs-PA

Synthesis of MNPs-IT-PA 4. To a solution of imidazole (6.8 g, 100 mmol) in dry toluene (100 mL), 3-chloropropyltriethoxysilane (24 mL, 100 mmol) was added in one portion. The reaction solution was refluxed for 24 h under nitrogen protection, And the mixture was evaporated under reduced pressure to remove the organic solvent. The residue was then purified with neutral alumina column chromatography (eluent: ethyl acetate) to give the intermediate **2**. 1.0 g of $SiO_2@ Fe_3O_4$ **1** (MNPs) was dispersed in 20 mL dry toluene by sonication for 1 h, and then the intermediate **2** (0.5 g) was added to the solution. After mechanical stirring under nitrogen atmosphere at reflux conditions for 48 h, the solid was magnetically separated and washed with ethanol, followed by drying under vacuum to afford Im-MNPs **3**. The resultant **3** (1.0 g) was dispersed in 50 mL dry ethanol by sonification for 1 h. 3-Bromopropylamine (0.27 g, 2.0 mmol) in 20 mL dry ethanol was added dropwise to the mixture and was further refluxed for 48 h under nitrogen protection. The solid catalyst MNPs-IT-PA **4** was collected by an external magnetic force, rinsed with ethanol, and then dried under vacuum for 6 h. Finally, 0.96 g grey nanoparticles (MNPs-IT-PA, **4**) were obtained with a loading of 0.34 mmol g^{-1}, as determined by elemental analysis.

Synthesis of MNPs-PA 6. 0.5 g of silica coated magnetic nanoparticles **1** (MNPs) was dispersed in dry toluene (30 mL) by ultrasonication for 5 min. (3-Aminopropyl)triethoxy silane (1.8 g) were added and the reaction mixture was refluxed for 12 h under nitrogen atmosphere. The supported catalyst MNPs-PA **6** was obtained by magnetic separation and washed with ethanol, and then dried in a vacuum oven at 60 °C for 6 h. The loading of the catalyst was determined to be 0.21 mmol g^{-1} by elemental analysis.

NMR data for intermediate 2. ^{1}H NMR (400 MHz, CDCl$_3$): δ 0.46–0.50 (m, 2H), 1.13–1.15 (m, 9H), 1.81 (t, $J = 8$ Hz, 2H), 3.74 (t, $J = 7.2$ Hz, 6H), 3.86 (t, $J = 7.2$ Hz, 2H), 6.84 (d, $J = 1.2$ Hz, 1H), 6.96 (s, 1H), 7.40 (s, 1H) ppm; ^{13}C NMR (100 MHz, CDCl$_3$): δ 7.3, 18.2, 24.8, 49.0, 58.4, 118.7, 129.2, 137.1 ppm.

4.4 General procedure for the MNPs-IT-PA catalyzed ambient Knoevenagel condensation in water

Benzaldehyde (5 mmol), methylene active compound (5 mmol), and MNPs-IT-PA (735 mg) were mixed in water (10 mL). The mixture was allowed to react at room temperature for a suitable length of time, which was decided by TLC. Separated from the reaction solution by a magnet, the catalyst was washed with ethanol and ethyl acetate, followed by drying under vacuum and reusing for subsequent runs. The decanted solution was directly filtered and the remaining residue was purified with recrystallization using ethanol or column chromatography using petroleum ether/ethyl acetate as the eluent. The products were characterized by ^{1}H NMR and ^{13}C NMR.

NMR data for representative products

2-(1H-Benzoimidazol-2-yl)-3-(thiophen-2-yl)acrylonitrile (Table 1, model reaction). ^{1}H NMR (400 MHz, CDCl$_3$): δ 7.15–7.22 (m, 1H), 7.30–7.37 (m, 2H), 7.50–7.52 (m, 1H), 7.66–7.70 (m, 2H), 7.76–7.77 (m, 1H), 7.87–7.89 (m, 1H), 8.63 (s, 1H) ppm; ^{13}C NMR (100 MHz, CDCl$_3$): δ 98.1, 115.6, 115.7, 116.7, 123.6, 129.1, 134.5, 136.8, 137.0, 139.3, 147.6 ppm.

2-(1H-Benzoimidazol-2-yl)-3-phenylacrylonitrile (Table 2, entry 1). ^{1}H NMR (400 MHz, CDCl$_3$): δ 7.31–7.34 (m, 2H), 7.50–7.52 (m, 3H), 7.65 (s, 2H), 7.98–7.80 (m, 2H), 8.51 (s, 1H) ppm; ^{13}C NMR (100 MHz, CDCl$_3$): δ 111.2, 116.8, 119.7, 123.6, 124.2, 129.3, 130.0, 132.1, 132.7, 146.3, 146.8 ppm.

2-(1H-Benzoimidazol-2-yl)-3-(3-methoxyphenyl)acrylonitrile (Table 2, entry 4). ^{1}H NMR (400 MHz, CDCl$_3$): δ 3.89 (s, 3H), 7.07–7.09 (m, 1H), 7.33–7.44 (m, 3H), 7.55–7.59 (m, 2H), 7.66 (s, 2H), 8.53 (s, 1H) ppm; ^{13}C NMR (100 MHz, CDCl$_3$): δ 55.5, 105.8, 114.1, 116.5, 119.0, 121.7, 123.4, 123.7, 126.0, 127.0, 130.2, 133.6, 135.0, 146.9, 153.6, 160.0, 162.7 ppm.

2-(1H-Indol-2-yl)-3-phenylacrylonitrile (Table 2, entry 15). ^{1}H NMR (400 MHz, CDCl$_3$): δ 7.28–7.33 (m, 2H), 7.41–7.49 (m, 4H), 7.60–7.63 (m, 2H), 7.88 (d, 2H, $J = 5.6$ Hz), 8.00 (d, 1H, $J = 6.0$ Hz) ppm, 8.58 (s, 1H); ^{13}C NMR (100 MHz, CDCl$_3$): δ 106.5, 112.4, 113.1, 118.9, 120.0, 121.5, 123.6, 124.4, 125.8, 128.9, 129.1, 129.8, 134.9, 137.3, 138.2 ppm.

2-(1H-Indol-2-yl)-3-p-tolylacrylonitrile (Table 2, entry 16). ^{1}H NMR (400 MHz, CDCl$_3$): δ 2.42 (s, 3H), 7.26–7.33 (m, 4H), 7.45 (d, 1H, $J = 6.4$ Hz), 7.57–7.60 (m, 2H), 7.79 (d, 2H, $J = 6.4$ Hz), 8.00 (d, 1H, $J = 6.0$ Hz), 8.46 (s, 1H) ppm; ^{13}C NMR (100 MHz, CDCl$_3$): δ 21.8, 105.3, 112.3, 113.3, 119.1, 120.0, 121.4, 123.5, 124.4, 125.4, 128.9, 129.8, 132.1, 137.2, 138.5, 140.2 ppm.

4-Methyl-3-oxo-N-phenyl-2-(phenylmethylene)pentanamide (Scheme 3, II). ^{1}H NMR (400 MHz, CDCl$_3$): δ 1.21 (d, 6H, $J = 6.4$ Hz), 3.36 (m, 1H), 7.14–7.18 (m, 1H), 7.32–7.38 (m, 5H), 7.47 (d, 2H, $J = 7.6$ Hz), 7.56–7.59 (m, 3H), 7.64 (s, 1H) ppm; ^{13}C NMR (100 MHz, CDCl$_3$): δ 19.1, 36.7, 120.3, 125.0, 129.0, 129.1, 130.0, 130.1, 133.0, 136.2, 137.4, 140.7, 165.5 ppm.

Acknowledgements

References

1 D. T. Mowry, *J. Am. Chem. Soc.*, 1945, **67**, 1050.

2 R. Trotzki, M. M. Hoffmann and B. Ontruschka, *Green Chem.*, 2008, **10**, 873.

3 Y.-F. Lai, H. Zheng, S.-J. Chai, P.-F. Zhang and X.-Z. Chen, *Green Chem.*, 2010, **12**, 1917.

4 W. Yu, S. Zhang, S. Ying, C. Zhao, S. Luo and C. Au, *Catal. Commun.*, 2011, **12**, 1333.

5 C. Mukhopadhyay and S. Ray, *Catal. Commun.*, 2011, **12**, 1496.

6 M. Zhang, P. Zhao, Y. Leng, G. Chen, J. Wang and J. Huang, *Chem.–Eur. J.*, 2012, **18**, 12773.

7 (*a*) A. Dandia, V. Parewa, A. K. Jain and K. S. Rathore, *Green Chem.*, 2011, **13**, 2135; (*b*) S. Sobhani, Z. P. Parizi and S. Rezazadeh, *J. Organomet. Chem.*, 2011, **696**, 813; (*c*) L. Tedeschi and D. Enders, *Org. Lett.*, 2011, **3**, 3515.

8 (*a*) L. E. Polander, S. Barlow, B. M. Seifried and S. R. Marder, *J. Org. Chem.*, 2012, **77**, 9426; (*b*) J. Mondal, A. Modak and A. Bhaumik, *J. Mol. Catal. A: Chem.*, 2011, **355**, 236; (*c*) S. B. Bharate, R. Mudududdla, J. B. Bharate, N. Battini, S. Battula, R. R. Yadav, B. Singh and R. A. Vishwakarma, *Org. Biomol. Chem.*, 2012, **10**, 5143; (*d*) J. Wang, Z. Zhang, W. Wang and F. Liu, *Org. Biomol. Chem.*, 2013, **11**, 2034.

9 (*a*) F. Liang, Y.-J. Pu, T. Kurata, J. Kido and H. Nishide, *Polymer*, 2005, **46**, 3767; (*b*) G. A. Kraus and M. E. Krolski, *J. Org. Chem.*, 1986, **51**, 3347; (*c*) F. Freeman, *Chem. Rev.*, 1980, **80**, 329.

10 (*a*) A. V. Narsaiah, A. K. Basak, B. Visali and K. Nagaiah, *Synth. Commun.*, 2004, **34**, 2893; (*b*) J. J. Han, Y. F. Xu, Y. P. Su, X. G. She and X. F. Pan, *Catal. Commun.*, 2008, **9**, 2077.

11 (*a*) M. B. Gawande and R. V. Jayaram, *Catal. Commun.*, 2006, **7**, 931; (*b*) G. Li, J. Xiao and W. Zhang, *Green Chem.*, 2012, **14**, 2234; (*c*) G. Li, J. Xiao and W. Zhang, *Green Chem.*, 2011, **13**, 1828; (*d*) Y. Wei, S. Zhang, S. Yin, C. Zhao, S. Luo and C. Au, *Catal. Commun.*, 2011, **12**, 1333; (*e*) V. S. R. R. Pullabhotla, A. Rahman and S. B. Jonnalaghadda, *Catal. Commun.*, 2009, **10**, 365; (*f*) L. Martins, W. Hölderich, P. Hammer and D. Cardoso, *J. Catal.*, 2010, **271**, 220; (*g*) F. X. L. Xamena, F. G. Cirujano and A. Corma, *Microporous Mesoporous Mater.*, 2012, **157**, 112.

12 See recently published reviews: (*a*) A. H. Lu, E. L. Salabas and F. Schüth, *Angew. Chem., Int. Ed.*, 2007, **46**, 1222; (*b*) M. B. Gawande, P. S. Branco and R. S. Varma, *Chem. Soc. Rev.*, 2013, **42**, 3371; (*c*) R. B. Nasir Baig and R. S. Varma, *Chem. Commun.*, 2013, **49**, 752.

13 B. Atashkar, A. Rostami and B. Tahmasbi, *Catal. Sci. Technol.*, 2013, **3**, 2140.

14 M. B. Gawande, A. K. I. D. Rathi, Nogueira, R. S. Varma and P. S. Branco, *Green Chem.*, 2013, **15**, 1895.

15 M. Lombardo and C. Trombini, *ChemCatChem*, 2010, **2**, 135.

16 A. Ying, S. Liu, Y. Ni, F. Qiu, S. Xu and W. Tang, *Catal. Sci. Technol.*, 2014, **4**, 2115.

17 X. Jin, D. Yang, X. Xu and Z. Yang, *Chem. Commun.*, 2012, **48**, 9017.

18 M. R. dos Santos, A. F. Gomes, F. C. Gozzo, P. A. Z. Suarez and B. A. D. Neto, *ChemSusChem*, 2012, **5**, 2383.

19 M. Lombardo, M. Chiarucci and C. Trombini, *Green Chem.*, 2009, **11**, 574.

20 Z.-H. Li, Z.-M. Zhou, X.-Y. Hao, J. Zhang, X. Dong and Y.-Q. Liu, *Chirality*, 2012, **24**, 1092.

21 S. S. Khan, J. Shah and J. Liebscher, *Tetrahedron*, 2011, **67**, 1812.

22 L. Dai, L. Yuan, X. Li, Z. Li, D. Xu, F. Fei, Y. Liu and J. Zhang, *Tetrahedron: Asymmetry*, 2011, **22**, 1379.

23 M. Lombardo, M. Chiarucci and C. Trombini, *Chem.–Eur. J.*, 2008, **14**, 11288.

24 (*a*) A. Ying, S. Xu, S. Liu, Y. Ni, J. Yang and C. Wu, *Ind. Eng. Chem. Res.*, 2014, **53**, 547; (*b*) A. Ying, H. Liang, R. Zheng, C. Ge, H. Jiang and C. Wu, *Res. Chem. Intermed.*, 2011, **37**, 579; (*c*) A.-G. Ying, L. Liu, G.-F. Wu, G. Chen, X.-Z. Chen and W.-D. Ye, *Tetrahedron Lett.*, 2009, **50**, 1653; (*d*) A.-G. Ying, X.-Z. Chen, C.-L. Wu, R.-H. Zheng, H.-D. Liang and C.-H. Ge, *Synth. Commun.*, 2012, **42**, 3455; (*e*) A. Ying, Y. Ni, S. Xu, S. Liu, J. Yang and R. Li, *Ind. Eng. Chem. Res.*, 2014, **53**, 5678; (*f*) S. Liu, Y. Ni, J. Yang, H. Hu, A. Ying and S. Xu, *Chin. J. Chem.*, 2014, **32**, 343.

25 (*a*) K. Nishioa, M. Ikedaa, N. Gokonb, S. Tsubouchi, H. Narimatsua, Y. Mochizuki, S. Sakamotoa, A. Sandhuc, M. Abe and H. Handa, *J. Magn. Magn. Mater.*, 2007, **310**, 2408; (*b*) Y. Jiang, C. Guo, H. Gao, H. Xia, I. Mahmood, C. Liu and H. Liu, *AIChE J.*, 2012, **58**, 1203.

26 Y. H. Deng, D. W. Qi, C. H. Deng, X. M. Zhang and D. Y. Zhao, *J. Am. Chem. Soc.*, 2008, **130**, 28.

27 (*a*) A. L. Morel, S. I. Nikitenko, K. Gionnet, A. Wattiaux, J. Lai-Kee-Him, C. Labrugere, B. Chevalier, G. Deleris, C. Petibois, A. Brisson and M. Simonoff, *ACS Nano*, 2008, **2**, 847; (*b*) Q. Zhang, H. Su, J. Luo and Y. Wei, *Green Chem.*, 2012, **14**, 201; (*c*) Q. Du, W. Zhang, H. Ma, J. Zheng, B. Zhou and Y. Li, *Tetrahedron*, 2012, **68**, 3577.

28 (*a*) X. Wang, P. P. Dou, P. Zhao, C. M. Zhao, Y. Ding and P. Xu, *ChemSusChem*, 2009, **2**, 947; (*b*) H.-J. Xu, X. Wan, Y.-Y. Shen, S. Xu and Y.-S. Feng, *Org. Lett.*, 2012, **14**, 1210.

29 Y. Zhang, Y. Zhao and C. Xia, *J. Mol. Catal. A: Chem.*, 2009, **306**, 107.

30 A. Bordoloi, S. Sahhoo, F. Lefebvre and S. B. Halligudi, *J. Catal.*, 2008, **259**, 232.

31 F. Nemati, M. M. Heravi and R. S. Rad, *Chin. J. Catal*, 2012, **33**, 1825.

32 G. Wang, N. Yu, L. Peng, R. Tan, H. Zhao, D. Yin, H. Qiu, Z. Fu and D. Yin, *Catal. Lett.*, 2008, **123**, 252.

33 Y. Kong, R. Tan, L. Zhao and D. Yin, *Green Chem.*, 2013, **15**, 2422.

34 (*a*) A. Graul and J. Castaner, *Drugs Future*, 1997, **22**, 956; (*b*) K. L. Baumann, D. E. Butler, C. F. Deering, K. E. Mennen, A. Millar, T. N. Nanninga, C. W. Palmer and B. D. Roth, *Tetrahedron Lett.*, 1992, **33**, 2283; (*c*) H. W. Lee, Y. M. Kim, C. L. Yoo, S. K. Kang and S. K. Ahn, *Biomol. Ther.*, 2008, **16**, 28.